

## IV.C.1c Multiply Surface-Functionalized Nanoporous Carbon for Vehicular Hydrogen Storage

P. Pfeifer (Primary Contact), C. Wexler,  
G. Suppes, F. Hawthorne, S. Jalisatgi, M. Lee,  
D. Robertson

University of Missouri  
223 Physics Building  
Columbia, MO 65211  
Phone: (573) 882-2335  
E-mail: pfeiferp@missouri.edu

DOE Technology Development Manager:  
Carole Read

Phone: (202) 586-3152  
E-mail: Carole.Read@ee.doe.gov

DOE Project Officer: Jesse Adams

Phone: (303) 275-4954  
E-mail: Jesse.Adams@go.doe.gov

Contract Number: DE-FG36-08GO18142

Subcontractor:

Midwest Research Institute, Kansas City, MO

Project Start Date: September 1, 2008

Project End Date: January 31, 2012

### Objectives

- Fabricate high-surface-area, multiply surface-functionalized carbon ("substituted materials") for reversible hydrogen storage with superior storage capacity (strong physisorption).
- Characterize materials and storage performance. Evaluate efficacy of surface functionalization, experimentally and computationally, for fabrication of materials with deep potential wells for hydrogen sorption (high binding energies).
- Optimize gravimetric and volumetric storage capacity by optimizing pore architecture and surface composition ("engineered nanospaces").

### Technical Barriers

This project addresses the following technical barriers from the Hydrogen Storage section of the Fuel Cell Technologies Program Multi-Year Research, Development and Demonstration Plan:

- (A) System Weight and Volume
- (B) System Cost
- (E) Charging/Discharging Rates

- (J) Thermal Management
- (P) Lack of Understanding of Hydrogen Physisorption and Chemisorption

### Technical Targets

This project aims at the development of surface-engineered carbons, made from corncob or other low-cost raw materials, which simultaneously host high surface areas, created in a multi-step process, and a large fraction of surface sites with high binding energies for hydrogen, created by surface functionalization with boron, iron, and lithium. Targets are surface areas in excess of 4,500 m<sup>2</sup>/g, average binding energies in excess of 12 kJ/mol, and porosities below 0.8, toward the design of materials that meet the following 2015 DOE hydrogen storage targets:

- Gravimetric storage capacity: 0.055 kg H<sub>2</sub>/kg system
- Volumetric storage capacity: 0.040 kg H<sub>2</sub>/liter system

### Accomplishments

- Validated H<sub>2</sub> performance of University of Missouri carbons (University of Missouri; National Renewable Energy Laboratory; "blind laboratory") to within ~ 5%.
- Manufactured B-substituted carbon by thermolysis of B<sub>10</sub>H<sub>14</sub>, with B:C = 1-7 wt% without compromising high surface areas.
- Observed significant changes of hydrogen adsorption on B-substituted samples subjected to neutron irradiation (fission tracks in carbon matrix from boron neutron capture). Irradiation shifted excess adsorption peak and slope at 80 K to lower pressures, consistent with an increase in binding energy and decrease in density of the saturated film. Irradiation did not change surface area or pore-size distribution. Estimated saturated film densities at 80 K and 50 bar were 3-8 times the density of unadsorbed hydrogen gas.
- Developed method to determine isosteric heats of adsorption at high coverage from Clausius-Clapeyron equation in a thermodynamically consistent way.
- Developed sub-nm pore structure characterization methods based on small-angle X-ray scattering (SAXS) [1], and incoherent inelastic neutron scattering [2].

- Built a large “library” of B-substituted and B-free carbon materials, generating a systematic study of the structure and performance of activated carbons under various processing conditions (KOH concentration, activation temperature, pyrolysis of B-carrying polymers). Demonstrates a wide spectrum of different behaviors, with excess adsorption peaks ranging from 20 bar to pressures way above 100 bar, including record excess storage capacity of 1.3wt% at room temperature.
- Found evidence from library that B-substitution and irradiation raises average binding energy to 9-11 kJ/mol (B:C = 1.4 wt%) and alters entire shape of adsorption isotherm (B:C = 1.7 wt%). *Ab initio* calculations of H<sub>2</sub>-(B,C) interactions and Grand Canonical Monte Carlo (GCMC) simulations gave  $E_B = 10-14$  kJ/mol at B:C = 10 wt% [3].



## Introduction

High-surface-area carbons from corncob, as developed by our team, show considerable promise for reversible onboard storage of hydrogen at high gravimetric and volumetric storage capacity. A current carbon has a gravimetric storage capacity of 0.11 kg H<sub>2</sub>/kg carbon at 80 K and 50 bar. This project is a systematic effort to achieve comparable results at 300 K, by increasing surface areas from currently ~3,000 m<sup>2</sup>/g to ~5,000 m<sup>2</sup>/g, and substituting carbon with boron and other elements that increase the binding energy for hydrogen. Current high surface areas and high binding energies are hosted by sub-nm pores (“nanopores”) created by chemical means. New surface area, created by fission tracks from boron neutron capture,  $^{10}\text{B} + n \rightarrow [^{11}\text{B}] \rightarrow ^7\text{Li} + ^4\text{He} + \gamma + 2.4 \text{ MeV}$ , traversing stacks of graphene sheets, will add as much as another 3,000 m<sup>2</sup>/g. Thus boron serves in two functions: (i) raise the binding energy by electron donation from H<sub>2</sub> to electron-deficient B; (ii) provide the platform for creation of additional surface area.

## Approach

The approach is an integrated fabrication, characterization, and computational effort. Structural characterization includes determination of surface areas, pore-size distributions, and pore shapes. Storage characterization includes measurements of hydrogen sorption isotherms and isosteric heats. Computational work includes adsorption potentials and simulations of adsorbed films for thermodynamic analysis of experimental isotherms. Comparison of computed and

experimental isotherms validates theoretical adsorption potentials and experimental structural data.

## Results

Figure 1 shows results for hydrogen excess adsorption (80 K, 303 K) for a selected group of seven samples with different sorption characteristics: (i) commercial reference sample MSC-30 (Maxsorb, Kansai Coke and Chemicals Co., Ltd); (ii) boron-free biocarbon, 3K-20100217; (iii) boron-doped unirradiated and irradiated biocarbons 3K-H6 (II, A), 3K-H6 (II, A) Irr, 3K\*-H6 (II, A) Irr, and HS;0B.

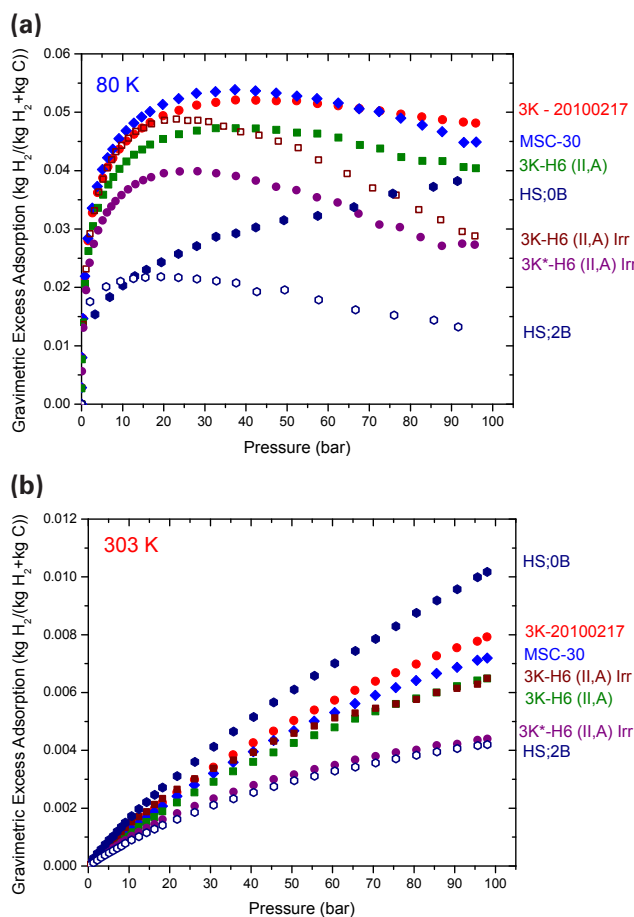


**FIGURE 1.** Gravimetric excess adsorption of H<sub>2</sub> on boron-substituted and boron-free samples at  $T = 80$  K (a) and 303 K (b). The samples exhibit a rich variety of different carbons and saturated film densities (Tables 1, 2), suggesting a broad potential for new materials with superior storage capacities. Excess isotherms at 80 K range from having a local maximum at a pressure of 21 bar (HS;2B) to pressures way above 100 bar (HS;0B). Samples MSC-30, 3K-20100217, 3K-H6 (II,A), 3K-H6 (II,A) Irr, 3K\*-H6 (II,A) Irr have high surface areas, 2,500-3,300 m<sup>2</sup>/g. Samples HS;0B and HS;2B have much lower surface areas, 600-700 m<sup>2</sup>/g; yet their gravimetric excess adsorption, especially HS;0B at 303 K, competes with, or outperforms, that of the high-surface carbons. Samples 3K-H6 (II,A), 3K-H6 (II,A) Irr, 3K\*-H6 (II,A) Irr, and HS;2B are boron-substituted; samples with “Irr” are irradiated samples. All isotherms are averages of multiple measurements.

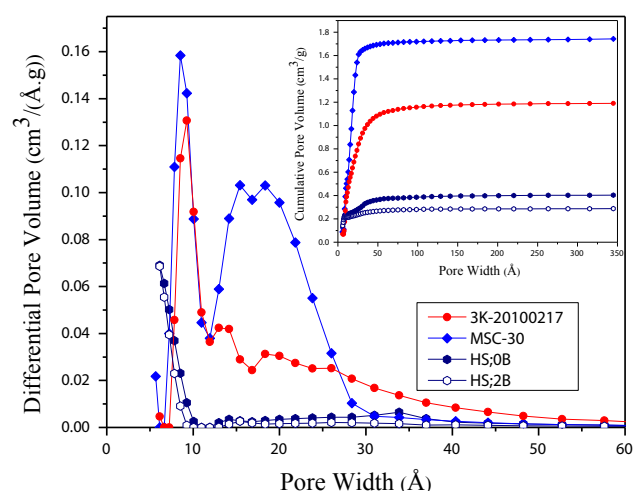


**FIGURE 2.** Differential and cumulative pore-size distributions for selected samples. Boron-free samples 3K-20100217 and MSC-30 contain a comparable number of sub-nm pores, but MSC-30 contains a significantly larger number of supra-nm pores. In contrast, PVDC samples, HS;0B (boron-free) and HS;2B (boron-substituted), are essentially free of supra-nm pores.

A) Irr, and 3K\*-H6 (II, A) Irr; and (iv) polyvinylidene chloride (PVDC)-based carbons HS;0B (0% B:C) and HS;2B (1.7 B:C). Sample 3K-20100217 is a member of a series of carbons, made from corncob, in which the ratio of potassium hydroxide (KOH) to carbon during chemical activation (treatment at 790°C) was varied from 2:1 (“2K”) to 6:1 (“6K”). Samples 3K and 3K\* differ in that the two were fabricated in a stainless-steel vessel, resulting in a ~1 wt% Fe and Cr content, and alumina, resulting in ~1 wt% Al. Boron doping was performed by vapor deposition followed by pyrolyzation of decaborane ( $B_{10}H_{14}$ ). Samples reported here were

exposed to air. Irradiated samples were produced at the University of Missouri Research Reactor, with irradiation times between 1 minute and 2 hours, and result in the production of fission tracks from boron neutron capture,  $^{10}B + n \rightarrow ^7Li + ^4He + \gamma + 2.4 \text{ MeV}$ . PVDC-based samples were formed by thermal decomposition of PVDC or PVDC co-polymerized with n-hexyl-ortho-carborane (samples were not further activated, all pores result from pyrolysis) [4]. Adsorption isotherm for sample 3K-20100217 at 77 K was validated at the National Renewable Energy Laboratory and a “blind laboratory,” resulting in an agreement in the excess adsorption to within a ~5% average relative error. Pore-size distributions (PSD) determined from  $N_2$  adsorption at 77 K (Figure 2) show that samples 3K-20100217 and MSC-30 contain a comparable number of sub-nm pores, but MSC-30 contains a significantly larger number of supra-nm pores. In contrast, PVDC samples, HS;0B and HS;2B, are essentially free of supra-nm pores. PSDs are consistent with SAXS analyses (Table 1, [1]). The existence of very narrow pores in HS;0B and HS;2B result in large binding energies [5] and explains the high room temperature excess adsorption of HS;0B (Figure 1), despite their low surface areas (Table 1). At low pressures HS;2B excess adsorption grows faster than HS;0B, indicating a number of high binding energy sites, as expected from our *ab initio* calculations of boron-containing carbons [3].

For irradiated samples, no significant differences in surface area or pore-size distribution between irradiated and unirradiated materials were found (Table 1, Figure 2). But significant differences in hydrogen adsorption isotherms at 80 K were observed (Figure 1). Irradiation shifted the maximum in excess adsorption from ~40 bar to ~20 bar, and made the slope at high pressures steeper (Figures 1, 3). The maxima,  $p_{\max}(T)$ ,

**TABLE 1.** Sample characteristic for selected materials. Specific surface areas, from Brunauer-Emmett-Teller analysis of  $N_2$  adsorption isotherms at 77 K and relative pressures 0.01-0.03, are rounded to nearest hundred. Porosities were determined from  $N_2$  adsorption at 77 K, at relative pressure 0.995 and by SAXS analysis [1]. Values for gravimetric excess adsorption,  $G_{\text{ex}}$  are presented at 80 K, 50 bar, and 303 K, 100 bar, and were determined using a standard skeletal density of 2.0 g/cm<sup>3</sup>.

Sample	Specific surface area, $\Sigma$ (m <sup>2</sup> /g)	Porosity from $N_2$ adsorption	Porosity from SAXS	Average nanopore width & length from SAXS (nm)	B:C (wt%), PGAA	Excess ads. (kg H <sub>2</sub> /(kg H <sub>2</sub> + kg C), 80 K, 50 bar)	Excess ads. (kg H <sub>2</sub> /(kg H <sub>2</sub> + kg C), 303 K, 100 bar)
MSC-30	2,600	0.79	0.76	0.6, 2.6	0.0%	0.053	0.0073
3K-20100217	2,500	0.78	0.77	0.6, 1.9	0.0%	0.065	0.0080
3K-H6 (II-A)	3,300	0.77	N/A	0.6, 2.5	1.4%	0.047	0.0065
3K*-H6 (II-A)	2,900	0.79	0.78	0.5, 4.0	1.9%	N/A	N/A
3K-H6 (II-A) Irr.	3,000	0.78	N/A	0.6, 2.4	1.4%	0.045	0.0065
3K*-H6 (II, A) Irr	2,900	0.79	N/A	N/A	1.9%	0.037	0.0044
HS;0B	700	0.41	N/A	N/A	0.0%	0.033	0.013
HS;2B	600	0.38	N/A	N/A	1.7%	0.020	0.0043

N/A – not available; PGAA – Prompt-gamma activation analysis

and intercepts with the pressure axis,  $p_0(T)$  (Figure 3), were related to the average binding energy,  $E_{B,av}$ , and mass density of the saturated film,  $\rho_{film}(T)$  using:

$$\rho_{film}(T) = m_{H_2} p_0(T) / (kT) \quad (1)$$

$$E_{B,av} = N_A kT \ln \left\{ \frac{p_0(T) - 2p_{max}(T)}{p_{max}(T)^2} [\sinh(h\nu / (2kT))]^3 [(8\pi m_{H_2})^3 (kT)^5 / h^6]^{1/2} \right\} \quad (2)$$

where  $m_{H_2}$ ,  $N_A$ ,  $k$ ,  $\nu$ , and  $h$  are the mass of a hydrogen molecule, Avogadro's number, Boltzmann's constant, the vibrational frequency of an adsorbed hydrogen molecule relative to the substrate, and Planck's constant,

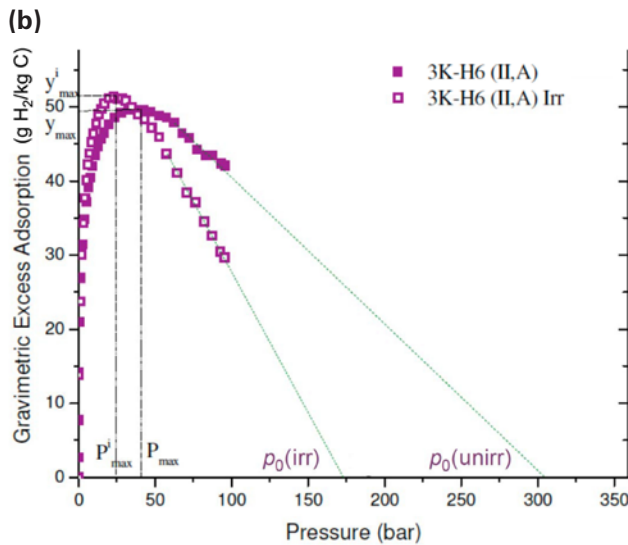
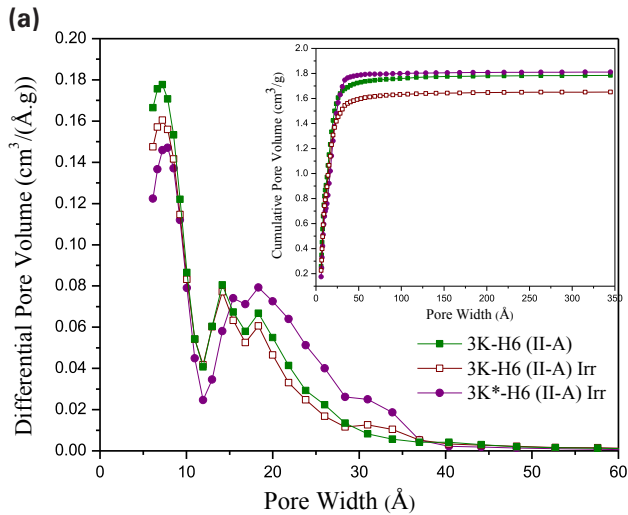


**FIGURE 3.** (a) Pore-size distributions for unirradiated and irradiated boron-doped samples. The difference between unirradiated and irradiated samples is considered insignificant. (b) Neutron irradiation of boron-doped sample 3K-H6 (II, A) shifts the maximum of excess adsorption isotherm,  $p_{max}$ , from ~40 bar to 24 bar and makes the slope of the isotherm steeper. Extrapolation of the linear part of the isotherm at high pressure gives the pressure,  $p_0$ , at which the hydrogen gas has the same density as the saturated adsorbed hydrogen film (see text and Eqs. 1, 2).

respectively, and we have assumed the ideal gas law, Eq. (1), and Langmuir adsorption, Eq. (2) [5]. Results are shown in Table 2. The increase in binding energy and decrease in film density as a result of irradiation were attributed to the creation of surface defects, perhaps free radicals, created by fission products, and film discontinuities at edges of fission tracks. Film densities at 80 K and 50 bar were 3-8 times the density of unadsorbed hydrogen gas (Table 2). The binding energies for B-substituted carbons inferred in Table 2, brackets, show that B-substitution raises the average binding energy to ~11 kJ/mol (B:C = 1.4 wt%) and alters entire shape of adsorption isotherm (B:C = 1.7 wt%; Figure 1). *Ab initio* calculations of  $H_2$ -(B,C) interactions and GCMC simulations gave  $E_B = 10$ –14 kJ/mol [3].

**TABLE 2.** Experimental density of the saturated  $H_2$  film at 80 K and average binding energy from Figures 1 and 3 and Eqs. (1, 2), with  $\nu$  for  $H_2$ -graphite potential and  $\nu$  estimated for  $H_2$ -B/C potential (in brackets).

Sample	$p_0$ (bar)	$p_{max}$ (bar)	$\rho_{film}$ (g/cm <sup>3</sup> )	B:C (wt%)	$E_{B,av}$ (kJ/mol)
MSC-30	360	~40	0.11	0.0%	6.4
3K-H6 (II,A)	300	~40	0.09	1.4%	6.2 (10.9)
3K-H6 (II,A) Irr	160	23	0.05	1.4%	6.5 (11.2)
3K*-H6 (II,A) Irr	190	24	0.06	1.9%	6.6 (11.3)
HS:2B	190	21	0.06	1.7%	6.9 (11.5)
H2 gas, 80 K & 50 bar	N/A	N/A	0.016	N/A	N/A

N/A – not available

The isosteric heat of adsorption,  $\Delta H$ , equals the heat released when a molecule is adsorbed at constant coverage (number of adsorbed molecules, absolute adsorption), and an according temperature change [6]. It is related to the binding energy through the relation  $\Delta H = E_{B,av} +$  zero-point/thermal energies =  $E_{B,av} + (3$ –5 kJ/mol), depending on the details of how  $H_2$  is adsorbed on the surface [7]. The isosteric heat can be computed from two adsorption isotherms via the Clausius-Clapeyron equation,

$$\Delta H = \frac{RT_1 T_2}{T_2 - T_1} \ln \left( \frac{p_2}{p_1} \right) \quad (3)$$

where  $p_i$ ,  $T_i$  are two pressures and temperatures corresponding to the same absolute adsorption. This requires conversion of experimental excess adsorption isotherm,  $G_{ex}$ , into absolute adsorption,  $G_{abs}$  (both in mass of  $H_2$  per mass of adsorbent),

$$G_{abs} = G_{ex} + \Sigma \cdot t_{film} \cdot \rho_{gas} \quad (4)$$

where  $\Sigma$ ,  $t_{film}$ , and  $\rho_{gas}$  are the specific surface area of the adsorbent (Table 1), thickness of the adsorbed film,

and density of bulk gas, respectively. In much of the literature, no distinction is made between absolute and excess adsorption, i.e., the conversion (4) is carried out with a film thickness of zero, and Eq. (3) is evaluated at constant excess adsorption instead of constant absolute adsorption. This leads to an incorrect behavior of isosteric heats at high coverage, where the film thickness is far from negligible: Whenever the excess adsorption isotherm has a local maximum in the pressure range analyzed (Figure 4a), the isosteric heat calculated from excess adsorption rises at high coverage (Figure 5a), which is unphysical. No such unphysical behavior occurs when isosteric heats are calculated from the absolute adsorption isotherm, which has no local maximum (Figure 4b). Figure 5a shows isosteric heats calculated for various hypothetical film

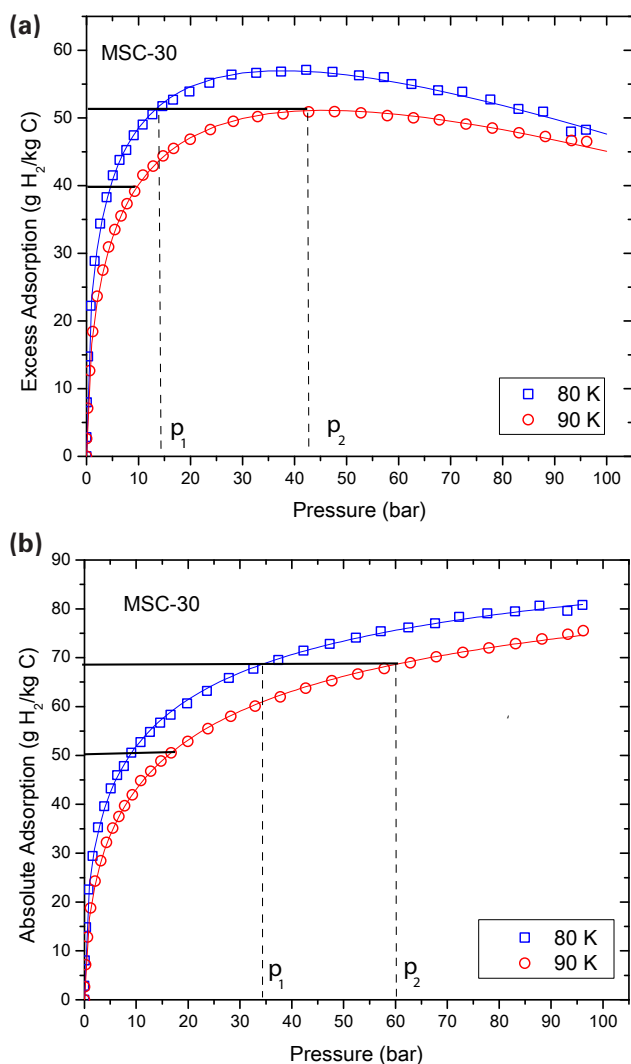


**FIGURE 4.** Determination of isosteric heats of adsorption from excess (a) and absolute (b) adsorption isotherms, from Eq. (4) with  $t_{\text{film}} = 4.1 \text{ \AA}$ . The maximum in the excess adsorption result in an unphysical rise of the isosteric heat (Figure 5).

thicknesses,  $t_{\text{film}} = 0$  (“ $G_{\text{abs}} = G_{\text{ex}}$ ”),  $t_{\text{film}} = 2.3 \text{ \AA}$  (van der Waals diameter), ...,  $t_{\text{film}} = 4.1 \text{ \AA}$  (best estimate from GCMC simulations of adsorbed H<sub>2</sub> on carbon surfaces). Significant differences in isosteric heats, due to incorrect values for  $t_{\text{film}}$ , are observed already at pressures as low as 2 bar (Figure 5a). The smallest film thickness at which the calculated isosteric heat curve no longer rises is a lower bound for the actual film thickness. Figure 5b displays the effect of different choices of the

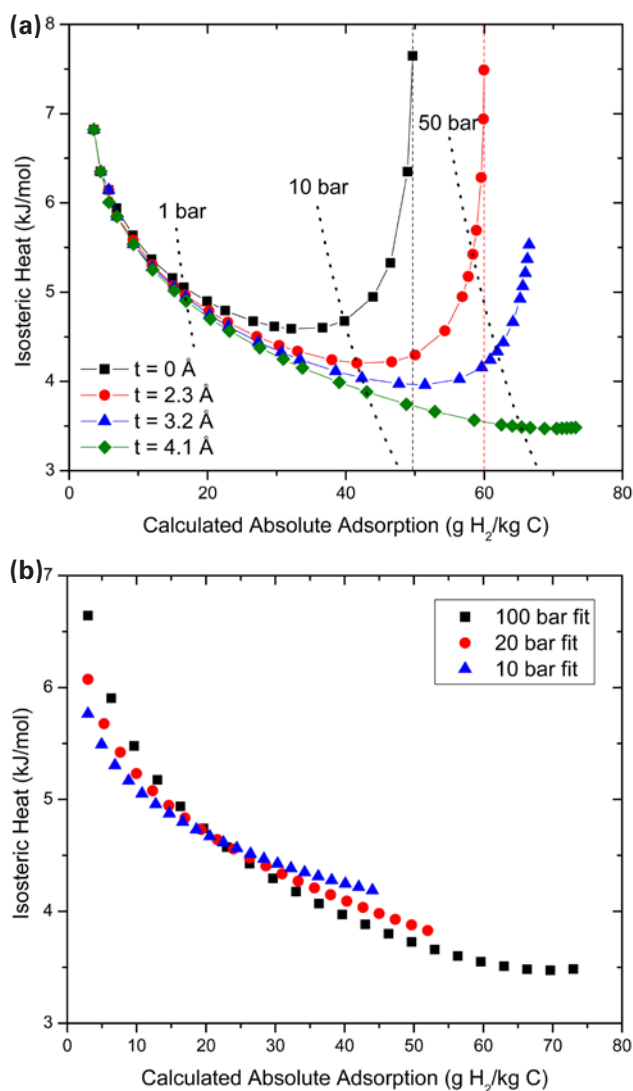


**FIGURE 5.** Isosteric heats of adsorption calculated from Eqs. (3, 4) for four different film thicknesses. (a) The increase in isosteric heat at high coverage is unphysical because high-energy adsorption sites are expected to fill at low coverage. The isosteric heat curves for  $t_{\text{film}} = 0$  and  $t_{\text{film}} = 2.3 \text{ \AA}$  end at  $G_{\text{abs}} \sim 50$  and  $\sim 60 \text{ g H}_2/\text{kg } ^\circ\text{C}$ , respectively, because the 80 K “absolute adsorption” isotherm for these film thicknesses has its maximum at  $\sim 50$  and  $\sim 60 \text{ g H}_2/\text{kg } ^\circ\text{C}$ . (b) Effect of different choices of the pressure interval over which absolute adsorption was fitted for interpolation (determination of  $p_1$  and  $p_2$  at constant coverage).

pressure interval over which absolute adsorption was fitted for interpolation (determination of  $p_1$  and  $p_2$  at constant coverage).

For the case study, MSC-30, isosteric heats drop from ~6 kJ/mol to ~3.5 kJ/mol as absolute adsorption increases from ~2 to ~70 g H<sub>2</sub>/kg °C. This is consistent with the expectation that sub-nm pores host binding energies as large as 10 kJ/mol, with larger pores hosting binding energies ~5 kJ/mol. The analysis also shows that isosteric heats from excess instead of absolute adsorption yield reliable values only at pressures below ~1 bar (Figure 5a). At the same time, isosteric heats at low pressures may differ by as much as 1 kJ/mol, depending on the pressure interval over which adsorption isotherms are fitted for interpolation (Figure 5b). Work is underway to determine isosteric heats on B-doped samples under oxygen-free conditions.

## Conclusions and Future Directions

- Observed an unexpected increase in binding energy and decrease in adsorbed film density/thickness in neutron-irradiated boron-containing carbons.
- Developed pore characterization methods using SAXS.
- Developed thermodynamically consistent method to determine isosteric heats at high coverage.
- Future work: (i) Construction of decaborane deposition and decomposition instrument to automate production of samples which will allow optimization of boron doping methods (time, temperature, decaborane concentration). (ii) Characterization of boron-free and boron-containing carbons under exclusion of oxygen and humidity. (iii) Etching of fission tracks to increase surface area and comparison of performance of etched/non-etched materials. (iv) Continue to investigate whether hydrogen and nitrogen see the same surface area. (v) Investigate pressure/temperature/pore shape dependence of new variable  $\rho_{\text{film}}(T)$  (density of saturated film) experimentally and by GCMC simulations. (vi) Design materials with high  $\rho_{\text{film}}(T)$ , as a concurrent strategy with increased binding energy. (vii) Improve theoretical models for analysis of excess adsorption isotherms ( $p_{\text{max}}, p_0, \partial G_{\text{ex}}/\partial p$ ) in terms of the binding energies and surface areas. (viii) Develop understanding of correlations between hydrogen storage at 80 K and 303 K. (ix) Expand experimental library of high  $E_{\text{B}}$  from boron doping (with extreme care to avoid exposure to oxidizing agents). (x) Attempt synthesis of bulk BC<sub>3</sub> and test for predicted H<sub>2</sub> intercalation.

## FY 2010 Publications/Presentations

1. R.J. Olsen, L. Firlej, B. Kuchta, H. Taub, P. Pfeifer, and C. Wexler, *Sub-Nanometer Characterization of Activated Carbon by Inelastic Neutron Scattering*, Carbon (Apr/2010, submitted).
2. C. Wexler, R. Olsen, P. Pfeifer, B. Kuchta, L. Firlej, Sz. Roszak, *Numerical Analysis of Hydrogen Storage in Carbon Nanopores*, Int. J. Mod. Phys. B (submitted Nov/2009, accepted, in press).
3. B. Kuchta, L. Firlej, Sz. Roszak, P. Pfeifer, and C. Wexler, *Influence of Structural Heterogeneity of Nano-Porous Sorbent Walls on Hydrogen Storage*, Appl. Surf. Sci. **256**, 5270–5274 (2010).
4. B. Kuchta, L. Firlej, R. Cepel, P. Pfeifer, and C. Wexler, *Structural and Energetic Factors in Designing a Nanoporous Sorbent for Hydrogen Storage*, Colloids and Surfaces A: Physicochem. Eng. Aspects **357**, 61–66 (2010).
5. P. Pfeifer, C. Wexler, G. Suppes, F. Hawthorne, S. Jalisatgi, M. Lee, and D. Robertson, *Multiply Surface-Functionalized Nanoporous Carbon for Vehicular Hydrogen Storage*, 2010 DOE Hydrogen Program Annual Merit Review, Washington, DC, June 7–11, 2010. Presentation D4.
6. *Technical Progress: H<sub>2</sub> storage and binding energies in high-surface-area nanoporous carbons*, Hydrogen Sorption Center of Excellence Face-to-Face Meeting, October 22–23, 2009. Presentation RC1-16.
7. L. Firlej, B. Kuchta, P. Pfeifer, and C. Wexler, *Adsorption of Hydrogen in Boron Substituted Carbon-Based Porous Materials*, 10<sup>th</sup> International Conference on Fundamentals of Adsorption (FOA10), Awaji, Hyogo, Japan, May 2010. Invited oral presentation.
8. R. Olsen, B. Kuchta, L. Firlej, P. Pfeifer, H. Taub, and C. Wexler, *Characterization of Sub-nm Pores in Carbon by Inelastic Neutron Scattering*, 10<sup>th</sup> International Conference on Fundamentals of Adsorption (FOA10), Awaji, Hyogo, Japan, May 2010. Poster.
9. C. Wexler, R. Olsen, M. Kraus, M. Beckner, B. Kuchta, L. Firlej, and P. Pfeifer, *High Storage Capacity of Hydrogen in Heterogeneous Carbon Nanopores: Experimental, Theoretical and Computational Characterization*, 10<sup>th</sup> International Conference on Fundamentals of Adsorption (FOA10), Awaji, Hyogo, Japan, May 2010. Poster.
10. C. Wexler, *Engineering a Nanoporous “Sponge” for Hydrogen Storage*, Colloquium, Department of Physics, University of Vermont, Burlington, VT, April 2010.
11. C. Wexler, *Hydrogen Absorption in Nanoporous Carbon*, Condensed Matter Seminar, Washington University, St. Louis, MO, April 2010.
12. C. Wexler, *A Brief History of Energy*, Public lecture in Saturday Morning Science (<http://satscience.missouri.edu>), Columbia, MO, February 2010.

13. C. Wexler, M. Beckner, J. Romanos, J. Burrell, M. Kraus, R. Olsen, E. Dohnke, S. Carter, G. Casteel, B. Kuchta, L. Firlej, E. Leimkuehler, A. Tekeei, G. Suppes, and P. Pfeifer, Record Hydrogen Storage Capacities in Advanced Carbon Storage Materials, *Bull. Am. Phys. Soc.* 55, T30.07 (2010).
  14. L. Firlej, B. Kuchta, Ss. Roszak, P. Pfeifer, and C. Wexler, *Adsorption of Hydrogen in Boron-Substituted Nanoporous Carbons*, *Bull. Am. Phys. Soc.* 55, T30.09 (2010).
  15. M. Beckner, R. Olsen, J. Romanos, J. Burrell, E. Dohnke, S. Carter, G. Casteel, C. Wexler, and P. Pfeifer, *Isosteric Heats of Adsorption for Activated Carbons Made from Corn Cob*, *Bull. Am. Phys. Soc.* 55, T30.10 (2010).
  16. R.J. Olsen, L. Firlej, B. Kuchta, P. Pfeifer, H. Taub, and C. Wexler, *Quantization of Adsorbed Hydrogen for Inhomogeneous Materials Characterization using Inelastic Neutron Scattering*, *Bull. Am. Phys. Soc.* 55, T30.11 (2010).
  17. M. Kraus, J. Ilavsky, M. Beckner, D. Stalla, C. Wexler, and P. Pfeifer, *Nanopore Structure from USAXS/SAXS in Advanced Carbon Materials for Hydrogen Storage*, *Bull. Am. Phys. Soc.* 55, T30.12 (2010).
  18. M. Kraus, C. Wexler, and P. Pfeifer, *Fractal Analysis of Boron Doped Activated Carbon*, *Bull. Am. Phys. Soc.* 55, T30.13 (2010).
  19. P. Pfeifer. *Nano research at MU-Physics*, The Missouri Nano Frontiers, Columbia, MO, November 2009. Invited talk.
  20. B. Kuchta, L. Firlej, R. Cepel, P. Pfeifer, and C. Wexler, *Structural and Energetic Factors in Designing a Perfect Nano-Porous Sorbent for Hydrogen Storage*, The Missouri Nano Frontiers, Columbia, MO, November 2009. Poster.
  21. R. Cepel, B. Kuchta, L. Firlej, P. Pfeifer, and C. Wexler, *Quantum Energy Levels of Hydrogen Adsorbed on Nanoporous Carbons*, The Missouri Nano Frontiers, Columbia, MO, November 2009. Poster.
  22. C. Wexler, *Hydrogen storage in engineered carbon nanospaces*, 2009 Physics Leaders Meeting, Department of Physics, University of Missouri, Columbia, MO, October 2009.
- ## References
1. M. Kraus, J. Ilavsky, M. Beckner, C. Wexler, and P. Pfeifer, *J. Appl. Cryst.*, submitted (2010).
  2. R.J. Olsen, L. Firlej, B. Kuchta, H. Taub, P. Pfeifer, and C. Wexler, *Carbon*, submitted (2010).
  3. L. Firlej, Sz. Roszak, B. Kuchta, P. Pfeifer, and C. Wexler, *J. Chem. Phys.* **131**, 164702 (2009).
  4. Work performed under a different project.
  5. J. Burrell *et al.*, *Nanotechnol.* **20**, 204026 (2009).
  6. W.A. Steele, *The Interaction of Gases with Solid Surfaces* (Pergamon Press, Oxford, 1974).
  7. Y.J. Chabal, In: *DOE Hydrogen Program, FY 2009 Annual Progress Report*, ed. S. Satyapal (U.S. Department of Energy, Washington, DC, 2009), p. 808-814.